PHILOSOPHICAL TRANSACTIONS B

royalsocietypublishing.org/rstb

Research

Cite this article: Rubenstein DR, Solomon J. 2026 Endocrine and epigenetic flexibility in an African starling. *Phil. Trans. R. Soc. B* **381**: 20250027.
https://doi.org/10.1098/rstb.2025.0027

Received: 23 May 2025
Accepted: 17 October 2025

One contribution of 17 to a theme issue 'Ecological epigenetics at the intersection of behaviour and life history variation in non-model animals'.

Subject Areas:
behaviour, genomics

Keywords:
phenotypic plasticity, phenotypic flexibility, glucocorticoids, corticosterone, epigenetics, DNA methylation

Author for correspondence:
Dustin R. Rubenstein
e-mail: dr2497@columbia.edu

Supplementary material is available online at
https://doi.org/10.6084/m9.figshare.c.8555982

THE ROYAL SOCIETY PUBLISHING

Endocrine and epigenetic flexibility in an African starling

Dustin R. Rubenstein and Joseph Solomon

Department of Ecology, Evolution & Environmental Biology, Columbia University, New York, NY, USA

DRR, 0000-0002-4999-3723

Although many organisms rapidly and repeatedly adjust their behaviour and physiology to cope with changing environmental conditions, it remains unclear which traits are expected to exhibit phenotypic flexibility, over what timescales, and in which environments. Here, we explore endocrine (glucocorticoid hormones) and epigenetic (DNA methylation) flexibility in superb starlings (*Lamprotornis superbus*), a species endemic to the savannas of East Africa but that also occurs less commonly in more arid and mesic habitats. After capturing individuals from three sites in central Kenya—desert margin, savanna bushland and forest margin—birds were housed for six months under common garden conditions in the field at the savanna site. We measured corticosterone (baseline, stress-induced) and quantified genome-wide DNA methylation at the time of initial capture, as well as after three and six months in captivity. The transition to captivity caused predictable increases in baseline—though not stress-induced—corticosterone and decreases in DNA methylation in genes related to development. After six months in captivity, baseline levels of corticosterone and most differentially methylated regions of the genome returned to pre-captive levels. Ultimately, this work shows that birds living in semi-arid environments exhibit flexible endocrine and epigenetic responses to the stress of captivity that reverse over time.

This article is part of the theme issue 'Ecological epigenetics at the intersection of behaviour and life history variation in non-model animals'.

1. Introduction

As environments become more unpredictable across much of the globe, it is critical to understand not only how organisms respond to environmental variation but also how these responses evolved [1]. One of the primary ways that organisms cope with environmental variation is through phenotypic plasticity, the ability to respond to environmental cues through the adjustment of genotypic expression, either during early life (termed irreversible or developmental plasticity) or throughout life (termed reversible plasticity or flexibility) [2,3]. Phenotypically flexible traits exhibit different phenotypes in different environments over the course of a lifetime, and some individuals can reversibly and repeatedly modify their phenotype in response to environmental change [4]. Yet, not all phenotypes are expected to be flexible because organisms are predicted to evolve different responses to environmental change according to the timescale of environmental variation and the degree of environmental predictability that they experience [5]. Moreover, even in the same species, some traits may be phenotypically flexible while others may not be. Determining which traits are flexible and which are not will therefore require a greater understanding of how different timescales of environmental variation shape phenotypic flexibility, as well as the genetic architecture and

molecular mechanisms that underlie phenotypic flexibility, particularly in organisms that experience varying environmental conditions over the course of their lifetime.

As physiological mediators linking behavioural responses to the environment, hormones respond dynamically and rapidly to changes in ecological or social conditions [6]. Hormones not only impact behavioural phenotypes, but as gene products themselves, they are a type of phenotypic trait, one that can change rapidly and flexibly as the environment changes. Endocrine flexibility is therefore the extent to which the hormonal response of an individual varies in scope or speed in relation to changing environmental stimuli [7,8]. Glucocorticoid hormones, including cortisol in mammals and corticosterone in birds, have been particularly well studied in the context of endocrine flexibility because they play a central role in regulating metabolism and homeostasis [9,10]. Although glucocorticoid hormones respond rapidly to changes in the ecological or social environment, the response can also be shaped by longer timescales of environmental variation [11]. It is therefore critical to determine which components of the glucocorticoid stress response are flexible and respond to rapidly changing environments or external stimuli, and which are not [7,8].

Although hormones link the expression of the genome to environmental stimuli, gene expression itself can be impacted by environmental stimuli via epigenetic changes, including the addition of a methyl group to cytosine DNA bases (DNA methylation), post-translational modification to histone proteins that shape the structure of chromatin (histone modification), or the regulatory actions of RNA molecules [12]. Epigenetic modifications such as DNA methylation can occur during development [13], as well as throughout life. For example, there is increasing evidence from taxa as diverse as mammals, birds and fish that DNA methylation can change rapidly and reversibly over time periods of minutes to months [14–17]. Yet, since not all of the genome is environmentally responsive, understanding which portions are developmentally plastic or phenotypically flexible will be critical for determining how environmental variation influences epigenetic change.

Here, we examined endocrine and epigenetic flexibility by measuring plasma corticosterone and DNA methylation from whole blood in superb starlings (*Lamprotornis superbus*) that were captured at three sites along an environmental gradient in central Kenya (desert margin, savanna bushland and forest margin) and subsequently housed under common garden conditions for six months at the savanna site. Superb starlings are endemic to the harsh and unpredictable environment of the semi-arid savannas of East Africa [18,19], but they are a cosmopolitan species that often associates with humans and whose range extends into both forest and desert margins. Annual variation in precipitation influences all aspects of the lives of superb starlings, including their physiology, life history, behaviour and fitness [18]. Previous work in this species suggests the potential for both endocrine and epigenetic flexibilities that are directly tied to variation in precipitation. For example, superb starlings sampled across an environmental gradient in Kenya differed in circulating corticosterone levels and adrenal sensitivity [11]. Although adrenal sensitivity appeared to be shaped more by long-term variation in precipitation, baseline corticosterone was influenced by both short- and long-term variations in rainfall, suggesting a flexible endocrine response to fluctuation in rainfall-driven resources [11]. Similarly, DNA methylation of the glucocorticoid receptor (*NR3C1*) in superb starlings also varied among chicks according to the amount of rainfall that their parents experienced prior to egg-laying, suggesting a potential role for developmental plasticity [20].

Our goal was to probe the mechanistic bases of environmental coping in this species by simultaneously studying physiological and molecular flexibility in the same individuals when moved from a natural setting to a more stressful setting in captivity. After birds were transferred from the wild to captivity, we wanted to (i) determine whether baseline and stress-induced corticosterone both exhibited phenotypic flexibility and (ii) identify environmentally responsive regions of the superb starling genome that exhibit epigenetic flexibility. Since previous work in this species has shown that birds at these three sampling sites differed in baseline and stress-induced corticosterone [11], we expected wild-caught birds to differ in their initial levels of corticosterone but then exhibit endocrine flexibility and converge on similar levels in captivity. Based on pilot work suggesting that superb starling corticosterone remains elevated for at least three months in captivity, we predicted an initial increase in both baseline and stress-induced corticosterone at three months in captivity owing to chronic stress, but then we expected levels to decline to wild levels by six months as birds became acclimated to captivity. Similarly, if superb starlings exhibit a flexible epigenetic response in DNA methylation to the chronic stress associated with being in captivity, we expected differences in some regions of the genome at three months in captivity that would begin to disappear by six months. Ultimately, the results of this study will help develop a framework for understanding the mechanistic bases of physiological and molecular flexibility in organisms living in changing and stressful environments.

2. Material and methods

(a) Field sampling

We sampled non-breeding adult superb starlings of both sexes in late June through July 2018 at three sites in central Kenya (supplementary material, table S1). The three sites (Merille, Timau and Mpala) were chosen based on known differences in their mean annual precipitation, their interannual variability in precipitation and their baseline corticosterone [11]. Merille (1° 25′ 1.4082″, 37° 43′ 21.8856″) lies on the southern edge of the Chalbi desert and experiences the lowest rainfall; Timau (0° 5′ 53.088″, 37° 14′ 27.204″) lies on the western slopes of Mount Kenya and experiences the highest rainfall; and Mpala (0° 19′ 25.4892″, 36° 54′ 11.4906″) lies on the Laikipia plateau in savanna bushland and experiences intermediate but highly unpredictable rainfall.

(b) Common garden experiment

In total, we captured 23 starlings (six from Merille, eight from Timau and nine from Mpala) using pull-string traps baited with papaya and maize meal [11]. Blood was collected from these birds immediately after capture in the wild, and then the birds were placed in three outdoor aviaries (2.5 × 1.5 × 2 m), where they were resampled two more times at three-month intervals (three-month and six-month post initial (wild) capture). Since superb starlings are highly social cooperative breeders [18], each aviary contained all of the birds captured from a single sampling site. Aviaries were covered with fibreglass board to exclude sun and direct precipitation, but otherwise experienced natural savanna conditions. Birds received ad libitum water and food daily (including papaya, cooked ground beef, maize meal and hard-boiled eggs). During each of the two sampling periods, birds in the aviaries were captured over a 3-day period at 05:00 to ensure that all birds were bled within 3 minutes of capture without first having been disturbed by activity. All of the birds in a single aviary were sampled on the same day, with the order of the three aviaries and the birds within them chosen arbitrarily. One bird died of natural causes during the experiment and could not be resampled at the six-month time period.

(c) Sample collection

From each individual, we collected a first blood sample from the brachial wing vein rapidly after capture to measure baseline corticosterone (mean time to collection ± s.e. = 115 ± 5.0 seconds, ranging from 42 to 215 seconds; 65 of 68 samples were collected within 180 seconds). A portion of this sample was preserved in 2% SDS Queen's lysis buffer for subsequent DNA extraction. We then restrained the birds in cloth bags for 30 minutes before a second blood sample was collected from the brachial vein to measure stress-induced corticosterone [11,21]. All blood samples were centrifuged in the field within 15 minutes of capture, and plasma drawn off with a syringe and frozen at −25°C at the Mpala Research Centre, before transport back to the USA on dry ice, where it was stored at −80°C until extraction. Blood samples in Queen's lysis buffer were stored in the refrigerator at 4°C until extraction (though transported to the USA at room temperature in less than 48 hours).

(d) Corticosterone analysis

Plasma corticosterone was measured with enzyme-linked immunosorbent assay (ELISA; Enzo Life Sciences, Farmingdale, NY) over six assay plates using a protocol previously validated for superb starlings [22]. Briefly, after plasma samples were thawed, we added 1% steroid displacement reagent 1 : 1 to each sample, before vortexing, and letting samples stand for 5 minutes. Each sample was then diluted 1 : 11 with assay buffer, and the kit's serial dilution corticosterone five-point standard curve tubes were prepared for each assay plate. Each plate included a standard curve (range: 32–20 000 $pgml^{-1}$) and two blank controls. The standard curve and the diluted samples were then pipetted into plate wells in duplicate, along with assay buffer into control wells. Blue conjugate and yellow antibody solutions were pipetted into each well, except appropriate control wells. Each plate was incubated on a plate shaker set to 500 rpm for 2 hours. Plates were then cleaned with wash buffer three times before undergoing a pNpp substrate reaction for 1 hour. Absorbance for each well was read at 405 nm using a plate reader (Bio-Rad, Hercules, CA). We calculated and corrected each sample's corticosterone concentration ($ngml^{-1}$) against the standard curve and controls. Sample order was randomized across plates, and intra- and inter-assay variability was also checked; intra- and inter-assay coefficients of variation were 6.7% and 12.6%, respectively. Redos of samples that lay off the standard curve were done at 1 : 40 dilution, as previously validated for this species [11].

Since two birds from Timau showed elevated corticosterone levels (both baseline and stress-induced) in all three sampling periods that were well outside the range of normal values [11], they were excluded from the hormone analysis (but included in the DNA methylation analysis; supplementary material, table S1). Both baseline and stress-induced corticosterone were analysed separately using general linearized mixed models (GLMMs), with sex, sampling site, sampling period, and the sampling site by sampling period interaction included as the dependent variables. Individual ID was also included in the models as a random effect to account for repeated sampling of the same individuals over time. *Post hoc* Tukey tests were used to compare groups. Both baseline and stress-induced corticosterone values were log transformed prior to analysis to meet assumptions of normality.

(e) Reduced representation bisulphite sequencing

DNA was extracted in 200 µl elutions from whole blood using a Qiagen DNAeasy Blood and Tissue kit (Qiagen, Hilden, Germany). From each elution, 80–120 ng was used to prepare libraries with a NUGen (acquired by Tecan, Männedorf, Switzerland) reduced representation bisulphite sequencing (RRBS) methyl-Seq kit. We spiked 1 ng unmethylated lambda (Promega cl857 Sam7) control DNA in each sample to evaluate successful bisulphite conversion. After an MspI digestion step at 37°C, followed by end repair and adapter ligation steps, Qiagen EpiTect Fast Bisulfite kits were used to convert the reactions to bisulphite DNA. Reactions were indexed with sequencing barcodes and amplified for 12 cycles at 60°C annealing temperature. Final libraries were purified with Agencourt DNA beads (Beckman Coulter, Brea, CA), quantified on a Qubit 3.0 Fluorometer, divided equally and equimolar balanced across four pools, and shipped on dry ice to the Novogene Corporation, Sacramento, CA. Each pool was quality checked on an Agilent 2100 Bioanalyzer and sequenced one pool per lane PE150 with 10% PhiX on an Illumina HiSeq 4000.

All 68 samples passed lambda control checks (mean = 0.43% methylated Cs for lambda genome alignments), but four samples had low coverage (fewer than 150 000 sequence pairs post-trimming) and were excluded from further analysis. The remaining

samples ranged from 3 103 858 to 49 287 711 sequence pairs (mean = 17 414 599), with bisulphite mapping efficiency from 41.3 to 75.90% (mean = 56.99%).

(f) Differentially methylated region analysis

Raw sequencing reads were trimmed with the Trim Galore v. 0.5.0 [23] wrapper for Cutadapt v. 1.18 [24] in paired-end mode using standard parameters for quality and adapter filtering, but with an additional 10 bp removed from the 5′ end from both read 1 and read 2 sequences to reduce M-bias as evaluated by Bismark Bisulfite Mapper v. 0.24.2 [25]. Reads were then trimmed again with NuGEN's trimRRBSdiversityAdaptCustomers Python script. Bismark was used to prepare a bisulphite version of the *L. superbus* reference genome CU_Lasu_v2 (GenBank Accession GCA_015883425.2) [26], and trimmed reads were aligned to this reference, with Bismark methylation extractor generating cytosine reports and CpG coverage outputs for each sample library. Reads were also aligned to the lambda genome to check bisulphite conversion rates.

CpG site coverage files were filtered at greater than or equal to 5× coverage and converted to sample bedgraphs with per cent DNA methylation for each CpG site at that coverage threshold across the genome. CpGs with at least 5× coverage ranged from 364 511 to 3 605 094 sites per sample, with a median coverage of 1 716 097 sites (supplementary material, table S2). Approximately 48% of the CpG sites were located within 10 kb of the transcription start site (TSS) of genes (hereafter, 10 kb putative promoters), and 24% occurred within gene bodies. These 5× sample bedgraphs were sorted and merged with bedtools v. 2.31.1 unionbedg [27]. We used Metilene v. 0.28 [28] to detect differentially methylated regions (DMRs) in pairwise group analyses between sampling periods (initial wild capture versus three months, wild versus six months and three months versus six months) with Metilene's default parameters. DMRs were minimum 10 CpG spans, with CpGs at a maximum distance from each other of 300 nt. Rather than ignore samples with missing sites, a minimum of 80% non-missing sample entries per CpG site in each group was used to estimate missing values from a beta distribution of non-missing values in each group. We report Benjamini–Hochberg (FDR) *p*-values. Bedtools was used to intersect significant DMRs from each comparison with 10 kb putative promoters and gene bodies. Geneious v. 10.0.4 was used to visually confirm DMRs in relation to genes. Bedtools was also used to map 5× CpG site averages for DMR regions associated with genes of interest. We also ran 10 randomized sample order Metilene runs for each of the three group comparisons to assess the relative abundance of called DMRs for actual sampling groups versus groups that may have occurred by chance.

Since we were interested in patterns of differential methylation across sampling periods, and given our sample size of only 23 individuals, we combined sexes and sampling sites for the DMR analysis. However, as described below, we included sex and sampling site as fixed effects (as well as individual ID and relatedness as random effects) in a GLMM testing CpG sites, and we report within-timepoint methylation means for sex and sampling site. Plots were created with ggplot2 v. 3.5.2 [29], forcats v. 1.0.0 [30], dplyr v. 1.1.4 [31] and viridis v. 0.6.5 [32] in R v. 4.5.1 [33].

(g) Variant calling on bisulphite sequencing alignments and relatedness matrix generation

Bismark alignment BAM files for the three-month samples were coordinate-sorted and given sample library information with Picard AddOrReplaceReadGroups v. 3.4.0 [34] for all individuals except for BB-17566 and BB-17585, where we used the higher read depth wild alignment files, and for BB-17565 and BB-17573, where we used the six-month alignment files because they generated more variant calls than the three-month versions for these samples. The sorted BAM files were converted into CGmap files with CGmapTools v. 0.1.3 [35] bam2cgmap function, and single nucleotide variants (SNVs) were called on the generated ATCGmap files with the Bayesian SNV mode, with dynamic *p*-values and with output set to all sites with a predictable genotype. Each sample library's VCF output was then compressed and indexed with bgzip and tabix v. 1.19 [36], and filtered with bcftools v. 1.19 [37] for biallelic single nucleotide polymorphisms (SNPs) with 'PASS' in the filter field at a format depth of 3, and then reheadered with sample/group names. Bcftools was then used to merge the 23 individual vcf.gz files, and fill allele total (AN) and allele count (AC) tags were added. Variants with a format depth of less than 10 or more than 500, and samples with more than 10% missing genotypes, were excluded. The merged file was then refiltered for 561 525 biallelic SNPs. The bcftools prune plugin was used to prune variants for linkage disequilibrium, with an r^2 of max 0.2 within a 1000-site window, leaving 502 SNPs.

PLINK v. 2.0.0-a.7LM AVX2 Intel [38,39] make-bed was used to create a PLINK binary output from the vcf.gz. These files were then loaded with GEMMA v. 0.98.5 [40] to estimate a centred relatedness matrix for the 23 birds, with a minimum allele frequency of 0.01 and Hardy–Weinberg test value of 0.001 (the PLINK .fam file was first filled with wild, three-month and six-month phenotypes as 1,2,3 in the sixth column, since GEMMA ignores samples with missing phenotypes).

(h) Assessing differentially methylated CpG sites within differentially methylated regions

The unfiltered Bismark coverage files were sorted, matched by site coordinates and merged for 61 samples across the wild, three-month and six-month sampling periods (excluding three samples that had less than 750 000 CpGs and sparse or no coverage in the Metilene DMR regions), resulting in 505 625 common CpG sites. We filtered for sites with a total count mean across samples greater than or equal to 10, leaving 502 035 sites, and then kept CpG sites with greater than 0 but less than 90 median methylation percentage (methylated sites/total sites). This resulted in 77 298 CpG sites, with 28 001 intersecting 10 kb putative promoters and 17 127 intersecting gene bodies.

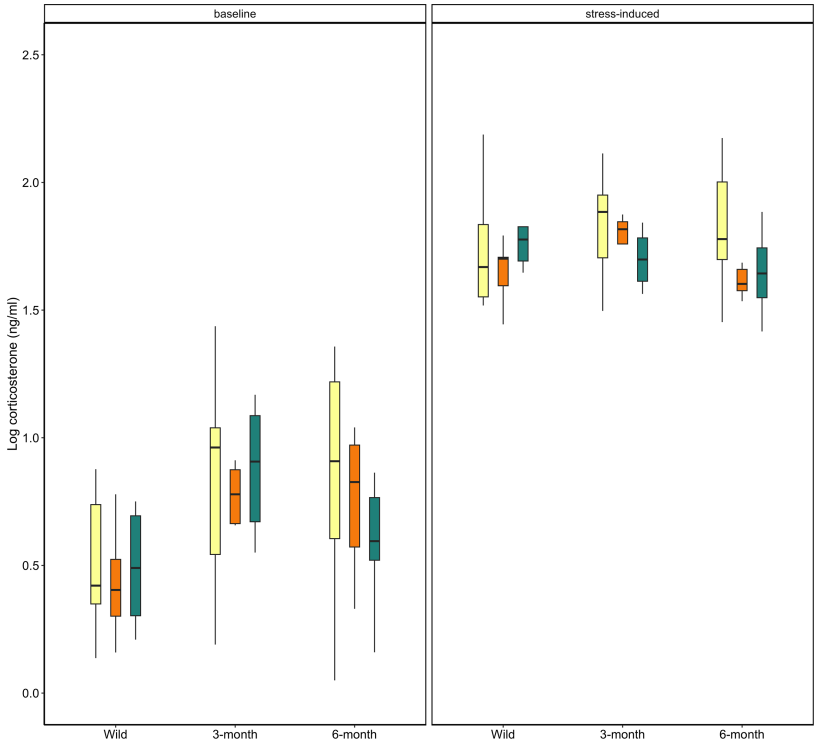

Figure 1. Comparison of baseline and stress-induced (30 minutes restrained) corticosterone for each of the three sampling periods in birds from Merille (yellow), Mpala (orange) and Timau (green). Baseline corticosterone did not differ among sites, but it did increase significantly from the wild to three months in captivity and then return to pre-capture levels by six months in captivity. There were no differences among sites or sampling periods in stress-induced corticosterone. Boxplots show median values with 25/75% quartiles, and whiskers are 1.5 times the interquartile range. For visualization, values were scaled as log corticosterone in ng/ml + 1.

Methylated and unmethylated count files for the 77 298 CpG sites were then loaded with sample attributes along with the GEMMA relatedness matrix (with any negative values zeroed to conform to a positive covariance matrix) using the R v. 4.5.1 environment package tidyverse v. 2.0.0 [41], Matrix v. 1.7.3 [42], multcomp v. 1.4.28 [43], and lme4 v. 1.1.37 [44] and its extension lme4qtl v. 0.2.2 [45] to fit a relmatGlmer GLMM based on the approach described in Lindner *et al.* [46]. For each CpG site, we included methylated and unmethylated counts as the binomial response variable, with sampling period (time_group for wild, three months and six months), sex and sampling site as fixed effects, as well as band (for each of the 23 birds) as a random effect to account for repeated measures, and the relatedness matrix by individual sample ID as an additional random effect. We used emmeans v. 1.11.2 [47] to create contrasts among time_groups, with unadjusted *p*-values. We then used the R package fdrtool v. 1.2.18 [48] to determine q-values for the unadjusted *p*-values generated by lme4qtl, and bedtools intersected significant (q-value less than 0.10) sites with the Metilene 10 kb putative promoter and gene body DMR ranges, as well as separately within the larger 10 kb putative promoter ranges (not only the DMR ranges) for genes associated with DMRs. Finally, we confirmed that no intersecting CpG sites failed to converge in GLMM.

3. Results

(a) Baseline corticosterone increased in captivity, but returned to pre-capture levels over time

Although the three sites did not differ in baseline corticosterone (even the initial wild-caught birds; $F_{2,57} = 0.11$, $p = 0.90$), we did find differences across the three sampling periods ($F_{2,57} = 3.59$, $p = 0.038$) (figure 1). Tukey tests revealed that baseline corticosterone levels increased significantly over the first three months in captivity ($p < 0.05$), but then began to decline by six months and did not differ from either wild ($p > 0.05$) or three-month levels ($p > 0.05$). Neither sex ($F_{1,57} = 0.13$, $p = 0.72$) nor the interaction between site and sampling period was significant ($F_{4,57} = 0.33$, $p = 0.86$). By contrast, stress-induced corticosterone did not differ between sites ($F_{2,57} = 0.91$, $p = 0.42$) or sampling periods ($F_{2,57} = 1.44$, $p = 0.25$), and neither sex ($F_{1,57} = 1.98$, $p = 0.18$) nor the interaction between site and sampling period was significant ($F_{4,57} = 1.86$, $p = 0.14$) (figure 1).

(b) DNA methylation declined in captivity, but returned to pre-capture levels over time

We identified 69 total DMRs, with eight DMRs within 10 kb putative promoters (we removed dual entries where DMRs were much closer to the TSS of nearest-neighbour genes for overlapping 10 kb putative promoters) and five DMRs within gene bodies in the wild versus three-month timepoint comparison, 16 total DMRs, with three DMRs within 10 kb putative promoters and two DMRs

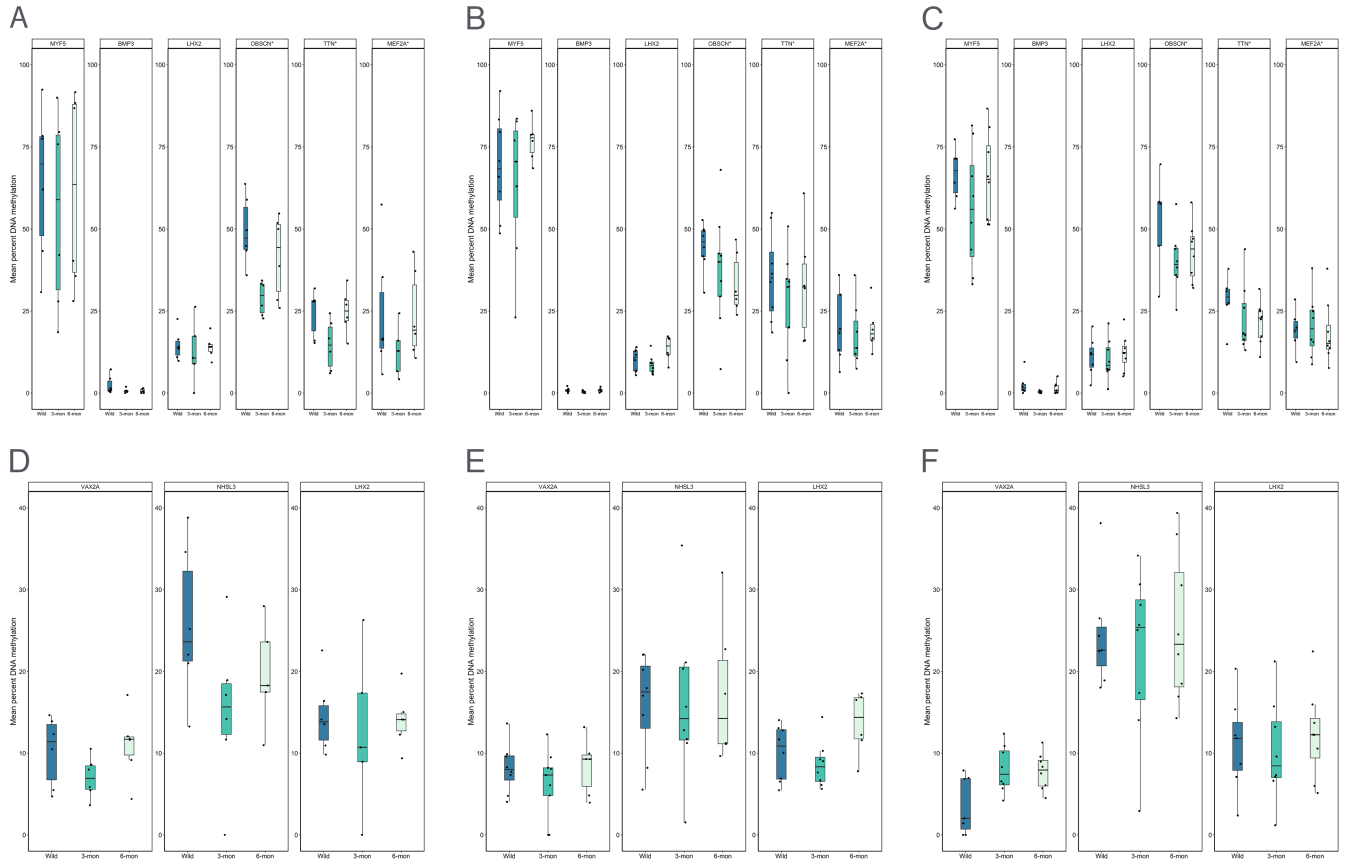

Figure 2. Mean percent DNA methylation for all 5× CpG sites within 10 kb putative promoter and gene body (noted with asterisk) DMR ranges for genes associated with developmental processes. Genes related to limb development and myogenesis in birds from (A) Merille, (B) Mpala and (C) Timau. Genes related to eye development in birds from (D) Merille, (E) Mpala and (F) Timau. DNA methylation tended to decline from the wild to three months in captivity, but then increase from three to six months in captivity. Boxplots show median values with 25/75% quartiles, and whiskers are 1.5 times the interquartile range.

within gene bodies in the wild versus six-month comparison, and 51 total DMRs, with 13 DMRs within 10 kb putative promoters and five DMRs within gene bodies in the three-month versus six-month comparison (table 1). In general, DNA methylation in most of these DMRs declined from the wild to the three-month sample, but then increased by the six-month sample. The majority of the DMRs occurred in genes related to development (table 1). In particular, a portion of these DMRs intersected with putative promoters and gene bodies for genes associated with myogenesis and limb and eye developmental processes (figure 2). We also found a prominent DMR in the putative promoter of *NPHP1*, a gene associated with kidney function (figure 3).

To determine if the DMRs that we identified in each of the comparisons were likely to be real or simply occurred by chance, we ran 10 randomized sample order Metilene runs for each of the three group comparisons. We identified an average of 14.9 DMRs for randomized wild versus three-month runs, an average of 28 DMRs for random wild versus six-month runs, and an average of 18.3 DMRS for randomized three-month versus six-month runs (supplementary material, table S3). For the wild versus three-month and three-month versus six-month comparisons, the DMR average was lower in randomized group-to-group contrasts than with actual contrasts, but in randomized wild versus six-month, the DMR average was more similar to the actual contrasts. Although regions with variable DNA methylation could be called DMRs by chance, the actual methylation patterns appeared more collectively directional in the wild versus three-month and three-month versus six-month comparisons. In addition, several developmental and muscle-related DMRs occurred together in the actual methylation results, though not together in the randomized results, providing additional confidence in our DMR calls.

(c) Individual CpG sites associated with differentially methylated regions showed similar methylation patterns

The lme4qtl binomial mixed model identified 6692 significant CpGs (after q-value correction with FDRtool) in the wild versus three-month contrast, 5608 significant CpGs in the wild versus six-month contrast and 5386 significant CpGs in the three-month versus six-month contrast (see supplementary material, table S4, and GLMM results). Of the 6692 CpGs in the wild versus three-month contrast, 4354 (65.1%) had lower three-month mean methylation than wild mean methylation; of the 5608 CpGs in the wild versus six-month contrast, 2833 (50.5%) had lower six-month mean methylation than wild mean methylation (a similar even pattern for the wild versus six-month to the randomized DMR results above); and of the 5386 CpGs in the three-month versus six-month contrast, 3691 (68.5%) had higher six-month mean methylation than three-month mean methylation. In other words, across

Table 1. List of DMRs detected in 10 kb putative promoters and gene bodies for each time period comparison (wild versus three-month, wild versus six-month, three-month versus six-month). Each DMR includes the chromosome number, the DMR start and stop sites, the number of CpG sites within each DMR, the mean methylation of each group and their difference, and the gene and its function.

region	chromosome number	DMR start site	DMR stop site	number of CpGs	mean methylation group 1	mean methylation group 2	mean methylation difference	gene	functional note (summary of NCBI gene and UniProt databases)
wild vs. 3-month									
10kb putative promoter	1A	19 628 016	19 628 063	14	61.99	51.11	10.89	MYF5	myogenic, limb development
	3	858 380	858 780	39	50.79	41.24	9.54	NPHP1	cilia, kidney function
	4	71 871 960	71 872 158	24	1.53	0.46	1.07	BMP3	limb development
	5B	4 112 829	4 113 111	35	23.27	16.50	6.77	AIP	cell process
	5B	4 114 989	4 115 023	12	31.92	19.17	12.75	CD163	macrophages
	19	7 955 801	7 955 923	17	21.75	17.32	4.43	IHE44_0007582 (unknown function)	glutamine-rich protein 2-like; possible sperm motility
	21	213 982	214 327	22	10.14	7.42	2.72	IHE44_0007780 (unknown function)	similar to SVBP and TMEM269
	unplaced (Contig 184)	880	902	10	40.03	31.73	8.30	PIM3	insulin secretion, response to glucose stimulus
gene body	5A	36 373 821	36 374 066	12	22.17	11.31	10.86	ACOT2	fatty acid oxidation in mitochondria
	7	14 984 161	14 984 330	15	27.35	19.67	7.68	TTN	striated muscles, mitosis
	7	21 997 057	21 997 095	11	42.96	31.71	11.25	OBSCN	myofibrillogenesis, striated muscle
	21	7 479 491	7 479 524	10	24.86	16.80	8.07	CA6	saliva protein
	27	2 041 175	2 041 224	15	3.10	1.90	1.21	IGHV	immunoglobulin
wild vs. 6-month									
10 kb putative promoter	3	858 352	858 472	28	39.70	35.19	4.51	NPHP1	cilia, kidney function
	4	2 296 927	2 297 548	14	7.74	10.24	−2.50	VAX2A	retinal development
	23	21 342	21 521	16	6.17	4.02	2.15	E2F2	transcription factor
gene body	26	6 577 147	6 577 210	19	13.76	23.43	−9.67	TRAF3IP3	innate immunity
	unplaced 36 (putative Chr 32)	765 539	765 584	10	7.46	14.76	−7.29	PCOLCE	procollagen
3-month vs. 6-month									
10 kb putative promoter	1A	19 628 024	19 628 063	13	51.78	66.30	−14.52	MYF5	myogenic, limb development
	3	480 133	480 257	10	28.31	36.02	−7.71	XRN2	transcription termination
	4	2 296 927	2 297 548	15	7.91	10.84	−2.93	VAX2A	retinal development
	5B	4 112 973	4 113 111	38	16.21	20.91	−4.69	AIP	cell process
	5B	4 114 975	4 115 023	14	19.85	33.37	−13.52	CD163	macrophages
	11	20 067 954	20 068 284	42	48.79	57.10	−8.31	GAS8	putative tumour suppressor

(Continued.)

Table 1. *(Continued.)*

region	chromosome number	DMR start site	DMR stop site	number of CpGs	mean methylation group 1	mean methylation group 2	mean methylation difference	gene	functional note (summary of NCBI gene and UniProt databases)
	14	2 965 165	2 965 332	23	4.56	8.06	−3.50	IHE44_0004115 (unknown function)	unknown
	14	15 224 394	15 224 771	23	33.28	42.59	−9.31	SEPT12	septin family of cytoskeletal GTPases
	17	357 227	357 372	23	18.55	24.96	−6.42	AJM1	apical junction
	17	10 144 052	10 144 092	14	9.03	13.58	−4.56	LHX2	limb, neural, corneal development, cell differentiation and development,
	23	1 727 821	1 727 995	20	16.41	23.19	−6.77	NHSL3	cell differentiation, cornea
	25	3 080 253	3 080 292	12	26.48	40.47	−13.99	S100A13	cell process
	28	2 364 283	2 364 314	12	38.79	55.04	−16.24	MAST3	cell process
gene body	2	294 603	294 866	15	17.60	25.11	−7.51	ATG9A	phospholipid scramblase activity
	5A	36 374 026	36 374 257	12	9.99	17.64	−7.66	ACOT2	fatty acid oxidation in mitochondria
	10	17 073 161	17 073 211	20	15.41	20.52	−5.11	MEF2A	transcription factor, muscle-specific, growth factor-induced and stress-induced genes
	25	3 080 253	3 080 292	12	26.48	40.47	−13.99	S100A13	cell process
	26	4 393 589	4 393 738	18	12.45	19.44	−6.98	PRELP	connective tissue

significant CpGs, the sampling period mean methylation trend strongly resembled the DMR sampling period mean methylation trend.

In addition to observing similar trends across sampling periods in the CpGs and DMRs, we also examined how the significant CpGs intersected with the DMRs ranges in both 10 kb putative promoters and gene bodies, and full 10 kb putative promoter ranges (i.e. not just the DMR ranges). For the wild versus three-month contrast, 75 CpGs intersected with Metilene 10 kb putative promoter DMRs, and 15 CpGs with Metilene gene body DMRs; for the wild versus six-month contrast, 20 CpGs intersected with 10 kb putative promoter DMRs, but zero CpGs with gene body DMRs; and for the three-month versus six-month contrast, 28 CpGs intersected with 10 kb promoter DMRs, and four with gene body DMRs. For the wild versus three-month contrast, 156 CpGs intersected with the larger (not just DMR range) 10 kb putative promoters of genes associated with DMRs; for the wild versus six-month contrast, 101 CpGs intersected with 10 kb putative promoters; and for the three-month versus six-month contrast, 87 CpGs intersected with 10 kb putative promoters. When each contrast's full significant CpG set (6692 for wild versus three-month, 5608 for wild versus six-month and 5386 for three-month versus six-month) was intersected with all 10 kb putative promoters, and allowed only one intersection per CpG (i.e. excluding overlapping promoters), the mean number of intersections per promoter region was 1.87 for wild versus three-month, 1.70 for wild versus six-month and 1.68 for three-month versus six-month. In comparison, the mean for wild versus three-month in DMR-associated promoters was 8.66 (min. of 1, max. of 53); the mean for wild versus six-month in DMR-associated promoters was 8.42 (min. of two, max. of 46); and the mean for three-month versus six-month in DMR-associated promoters was 4.83 (min. of one, max. of 24) (table 2). On the whole, CpGs significant in the GLMM for all three timepoints (but with timepoint contrasts) clustered more than average in the Metilene DMR ranges and associated promoters. For these CpGs, sampling period group mean methylation within sexes and sampling sites tended to follow the full timepoint group trends (see supplementary material, table S5, for CpG site intersects and means of mean methylation by timepoint, as well as means within sexes and sampling sites, and full methylation ratios for the 77 298 CpGs tested in the GLMM).

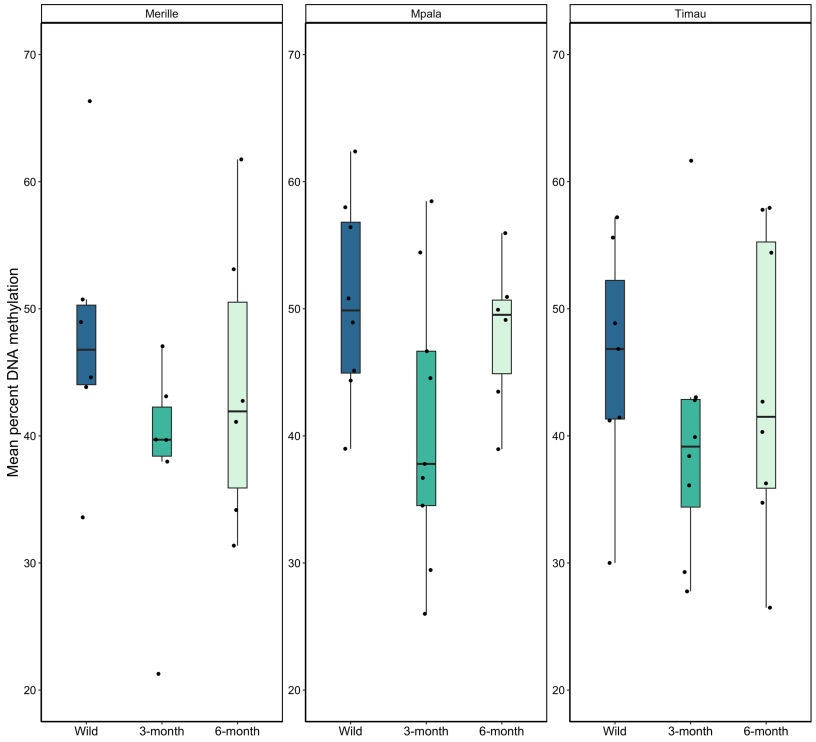

Figure 3. Mean percent DNA methylation for all 5× CpGs sites within 10 kb putative promoter DMR ranges for *NPHP1* in birds from each of the three sampling sites. DNA methylation tended to decline from the wild to three months in captivity, but then increase from three to six months in captivity. Boxplots show median values with 25/75% quartiles, and whiskers are 1.5 times the interquartile range.

Table 2. Summary of GLMM significant CpG intersects for DMRs (A) within 10 kb putative promoters, (B) within gene bodies, and (C) within full 10 kb putative promoter ranges for DMR-associated genes.

A		
	10 kb putative promoter DMR intersects	**10 kb putative promoter DMR intersects by gene**
wild vs. 3-month	75	9 MYF5, 31 NPHP1, 7 AIP, 11 CD163, 6 IHE44_0007582, 1 IHE44_0007780, 10 PIM3
wild vs. 6-month	20	20 NPHP1
3-month vs. 6-month	28	5 MYF5, 6 CD163, 1 GAS8, 5 IHE44_0004115, 3 AJM1, 4 NHSL3, 1 S100A13, 3 MAST3
B		
	gene bodies DMR intersects	**gene bodies DMR intersects by gene**
wild vs. 3-month	15	3 ACOT2, 2 TTN, 1 OBSCN, 9 CA6
wild vs. 6-month	0	0
3-month vs. 6-month	4	1 ACOT2, 1 MEF2A, 1 S100A13, 1 PRELP
C		
	10 kb promoter intersects	**10 kb putative promoter intersects by gene**
wild vs. 3-month	156	10 MYF5, 1 XRN2, 53 NPHP1, 2 VAX2A, 1 BMP3, 8 AIP, 26 CD163, 6 GAS8, 4 IHE44_0004115, 5 SEPT12, 2 AJM1, 6 IHE44_0007582, 1 IHE44_0007780, 1 E2F2, 4 NHSL3, 1 S100A13, 2 MAST3, 23 PIM3
wild vs. 6-month	101	46 NPHP1, 2 BMP3, 4 AIP, 14 CD163, 2 GAS8, 2 SEPT12, 4 AJM1, 3 IHE44_0007582, 2 IHE44_0007780, 3 NHSL3, 2 S100A13, 17 PIM3
3-month vs. 6-month	87	6 MYF5, 1 XRN2, 24 NPHP1, 1 VAX2A, 2 BMP3, 1 AIP, 13 CD163, 5 GAS8, 5 IHE44_0004115, 4 SEPT12, 5 AJM1, 2 IHE44_0007582, 1 IHE44_0007780, 1 E2F2, 4 NHSL3, 1 S100A13, 5 MAST3, 6 PIM3

4. Discussion

Superb starlings have been shown to exhibit differences in corticosterone and adrenal sensitivity across a country-spanning aridity gradient [11]. Here, we demonstrate that birds collected from three of the sites along this environmental gradient and housed under common garden conditions for six months showed similar increases in baseline (but not stress-induced) corticosterone after three months that then began to return to pre-capture levels by six months. As predicted from previous work showing that baseline corticosterone is influenced by annual variation in precipitation [11,21], baseline corticosterone appears to represent a flexible response to short-term environmental variation. Yet, stress-induced levels did not change over the duration of this study, a pattern also consistent with previous work showing that stress-induced corticosterone was poorly explained by precipitation variation on any timescale [11]. Although we did not observe any site differences in baseline corticosterone levels, these three particular sites did differ in baseline levels in a previous study [11]. This result underscores the dynamic nature of baseline glucocorticoid levels in general, and could be explained by annual differences in climatic conditions at the time of capture or the smaller sample sizes in this study. Such individual flexibility in the endocrine system, and in glucocorticoids in particular, is generally expected in changing environments [8]. The rapid and flexible response to the chronic stress of being held in captivity likely reflects an adaptation to dealing with the unpredictable environment associated with living in the East African savanna [19].

Environmental conditions, particularly during development, have long been known to influence DNA methylation [13,49]. In superb starlings, rainfall variation in early life was shown to influence DNA methylation in the glucocorticoid receptor, suggesting a role for developmental plasticity [20]. Increasingly, however, there is evidence that DNA methylation can also change rapidly over ecologically relevant timescales to the life of an organism and act as a phenotypically flexible trait. Three-spined stickleback [14] and Atlantic salmon [15] exhibited changes in DNA methylation in just a few days in response to salinity and thermal stress, and tree swallows exhibited changes in DNA methylation in response to corticosterone treatment in a few weeks [17]. Moreover, Trinidadian guppies showed changes in DNA methylation in response to anti-predator-inducing alarm cues in less than an hour [50]. Here, we observed changes in DNA methylation within three months for birds housed under common garden conditions in the field. We identified a series of DMRs related to development, most of which declined in the first three months in captivity, but then increased by six months to match pre-capture levels. Many of these DMRs occurred in genes related to limb and eye development. Myogenic factor 5 (*MYF5*) has been studied in avian and murine embryonic limb myogenesis [51,52], and bone morphogenetic protein 3 (*BMP3*) has similarly been linked to wing bud formation during chondrogenesis [53]. Although *BMP3* had overall low levels of DNA methylation in our study, the wild to three-month to six-month variation pattern was consistent across all three sampling sites (figure 2A–C). In addition, LIM Homeobox 2 (*LHX2*) has been extensively studied in the context of stem cell differentiation, including haematopoiesis [54,55], hair follicle specification [56], neurogenesis, forebrain/cortex and pituitary and limb development [57–62], as well as in retinal field and progenitor cell development [63–66]. Ventral anterior homeobox 2 (*VAX2A/VAX2*) had a methylation pattern similar to *LHX2* and is also associated with retinal development in chickens, African frogs, fruit flies, mice and humans [67–70]. The function of NHSL3/KIAA1522 is less well understood, but has recently been linked to endothelial corneal dystrophy in humans [71]. Finally, of particular interest was the gene Nephrocystin 1 (*NPHP1*), which had a very consistent methylation pattern across all three sampling sites (figure 3) and is associated with renal, photoreceptor and respiratory cilia, as well as with nephronophthisis, a disorder of the kidney [72–74].

To observe such consistent changes in DNA methylation in genes related to development from whole blood suggests that chronic stress may rapidly, though reversibly, alter developmental pathways in birds in ways that leave markers in the blood. Using DNA methylation in blood as a biomarker for epigenetic activity in the brain works well in some species but not in others [75]. For example, studies in the great tit have shown similar patterns of DNA methylation in the whole brain and blood [76], as well as between blood and liver [77]. In house sparrows, some patterns of DNA methylation are maintained across blood and brain tissues, particularly in genes for glucocorticoid and related receptors [78]. Here, we did not have permission to destructively sample birds, nor did we want to because our goal was to collect repeated samples from the same individuals over a six-month period. Nonetheless, our work highlights a suite of development-related genes that should prove useful for further study in additional species and tissue types.

Our common garden field experiment with superb starlings sampled across an environmental gradient in Kenya suggests that chronic stress associated with captivity causes predictable changes in baseline corticosterone that are consistent across birds from all sampling sites. In addition, birds in captivity for three months showed a decrease in DNA methylation in a suite of genes related to development. As birds became more accustomed to captivity by six months, both baseline corticosterone and DNA methylation in most of the DMRs returned to pre-captive levels. Thus, our study suggests that birds exhibit endocrine flexibility and respond to the chronic stress of being in captivity by increasing corticosterone levels for extended periods of time [8], and that this chronic stress may also impact DNA methylation in key developmental genes. These changes in DNA methylation were also flexible, and most DMRs returned to pre-captive levels of DNA methylation by the end of the experiment. Whether there is a direct relationship between corticosterone and DNA methylation, as there is in some avian species [17], remains to be studied. Future work should explore changes in DNA methylation over more rapid time courses (days to weeks rather than months), and more directly relate changes in DNA methylation to changes in corticosterone, particularly for the suite of developmental genes identified here. Ultimately, this work shows that birds living in a semi-arid environment exhibit flexible endocrine and epigenetic responses to the stress of captivity that begin to subside over time. Such rapid and reversible responses are likely to be adaptive and help these birds cope with the harsh and unpredictable environment of the East African savanna.

Ethics. This work was approved by Columbia University's Institutional Animal Care and Use Committee (IACUC protocol #AC-AAAW6451), as well as by the Kenyan National Commission for Science, Technology and Innovation, the Kenyan National Environmental Management Authority, the Kenya Wildlife Service, the Kenyan Wildlife Research and Training Institute and the Mpala Research Centre.

Data accessibility. Raw RRBS FASTQ sequences are available on the National Center for Biotechnology Information (NCBI) Sequence Read Archive [79]. Hormone data are available in the supplementary tables. Code for data processing steps is available on Dryad [80].

Supplementary material is available online [81].

Declaration of AI use. We have not used AI-assisted technologies in creating this article.

Authors' contributions. D.R.R.: conceptualization, funding acquisition, investigation, methodology, project administration, writing—original draft, writing—review and editing; J.S.: formal analysis, methodology, visualization, writing—review and editing.

Both authors gave final approval for publication and agreed to be held accountable for the work performed therein.

Conflict of interest declaration. We declare we have no competing interests.

Funding. This work was funded by a grant from the US National Science Foundation (IOS-1656098) to D.R.R.

References

1. Botero CA, Weissing FJ, Wright J, Rubenstein DR. 2015 Evolutionary tipping points in the capacity to adapt to environmental change. *Proc. Natl Acad. Sci. USA* **112**, 184–189. (doi:10.1073/pnas.1408589111)
2. Piersma T, Drent J. 2003 Phenotypic flexibility and the evolution of organismal design. *Trends Ecol. Evol.* **18**, 228–233. (doi:10.1016/S0169-5347(03)00036-3)
3. West-Eberhard MJ. 2003 *Developmental plasticity and evolution*. Oxford, UK: Oxford University Press.
4. Stager M, Velotta JP, Cheviron ZA, Senner NR. 2024 Assessing the evidence for treating developmental plasticity and phenotypic flexibility as different phenomena. *Funct. Ecol.* **39**, 2949–2961. (doi:10.1111/1365-2435.14590)
5. Wingfield JC, Sapolsky RM. 2003 Reproduction and resistance to stress: when and how. *J. Neuroendocrinol.* **15**, 711–724. (doi:10.1046/j.1365-2826.2003.01033.x)
6. Grindstaff JL, Beaty LE, Ambardar M, Luttbeg B. 2022 Integrating theoretical and empirical approaches for a robust understanding of endocrine flexibility. *J. Exp. Biol.* **225**, jeb243408. (doi:10.1242/jeb.243408)
7. Taff CC, Vitousek MN. 2016 Endocrine flexibility: optimizing phenotypes in a dynamic world? *Trends Ecol. Evol.* **31**, 476–488. (doi:10.1016/j.tree.2016.03.005)
8. Sapolsky RM, Romero LM, Munck AU. 2000 How do glucocorticoids influence stress responses? Integrating permissive, suppressive, stimulatory, and preparative actions. *Endocr. Rev.* **21**, 55–89. (doi:10.1210/edrv.21.1.0389)
9. McEwen BS, Wingfield JC. 2003 The concept of allostasis in biology and biomedicine. *Horm. Behav*. **43**, 2–15. (doi:10.1016/S0018-506X(02)00024-7)
10. Guindre-Parker S, Rubenstein DR. 2021 Long-term measures of climate unpredictability shape the avian endocrine stress axis. *Am. Nat.* **198**, 394–405. (doi:10.1086/715628)
11. Bird A. 2007 Perceptions of epigenetics. *Nature* **447**, 396–398. (doi: 10.1038/nature05913)
12. Weaver IC *et al.* 2004 Epigenetic programming by maternal behavior. *Nat. Neurosci.* **7**, 847–854. (doi:10.1038/nn1276)
13. Artemov AV *et al.* 2017 Genome-wide DNA methylation profiling reveals epigenetic adaptation of stickleback to marine and freshwater conditions. *Mol. Biol. Evol.* **34**, 2203–2213. (doi:10.1093/molbev/msx156)
14. Beemelmanns A *et al.* 2021 DNA methylation dynamics in Atlantic salmon (*Salmo salar*) challenged with high temperature and moderate hypoxia. *Front. Mar. Sci.* **7**, 604878. (doi:10.3389/fmars.2020.604878)
15. Lea AJ, Altmann J, Alberts SC, Tung J. 2015 Resource base influences genome-wide DNA methylation levels in wild baboons (*Papio cynocephalus*). *Mol. Ecol.* **25**, 1681–1696. (doi:10.1111/mec.13436)
16. Taff CC, McNew SM, Campagna L, Vitousek MN. 2024 Corticosterone exposure is associated with long-term changes in DNA methylation, physiology and breeding decisions in a wild bird. *Mol. Ecol.* **33**, ee17456. (doi:10.1111/mec.17456)
17. Rubenstein DR. 2016 Superb starlings: cooperation and conflict in an unpredictable environment. In *Cooperative breeding in vertebrates: studies of ecology, evolution, and behavior* (eds WD Koenig, JL Dickinson), pp. 181–196. Cambridge, UK: Cambridge University Press.
18. Rubenstein DR, Lovette IJ. 2007 Temporal environmental variability drives the evolution of cooperative breeding in birds. *Curr. Biol.* **17**, 1414–1419. (doi:10.1016/j.cub.2007.07.032)
19. Rubenstein DR, Skolnik HE, Berrio A, Champagne F, Phelps S, Solomon J. 2016 Sex-specific fitness effects of unpredictable early life conditions are associated with DNA methylation in the avian glucocorticoid receptor. *Mol. Ecol.* **25**, 1714–1728. (doi:10.1111/mec.13483)
20. Rubenstein DR. 2007 Stress hormones and sociality: integrating social and environmental stressors. *Proc. R. Soc. B* **274**, 967–975. (doi:10.1098/rspb.2006.0051)
21. Guindre-Parker S, Rubenstein DR. 2018. No short-term physiological costs of offspring care in a cooperatively breeding bird. *J. Exp. Biol.* **221**, jeb186569. (doi:10.1242/jeb.186569)
22. Martin M. 2011 Cutadapt removes adapter sequences from high-throughput sequencing reads. *EMBnet J.* **17**, 10–12. (doi:10.14806/ej.17.1.200)
23. Krueger F, Andrews SR. 2011 Bismark: a flexible aligner and methylation caller for bisulfite-Seq applications. *Bioinformatics* **27**, 1571–1572. (doi:10.1093/bioinformatics/btr167)
24. Rubenstein DR, Corvelo A, MacManes MD, Maia R, Narzisi G, Rousaki A, Vandenabeele P, Shawkey MD, Solomon J. 2021 Feather gene expression elucidates the developmental basis of plumage iridescence in African starlings. *J. Hered.* **112**, 417–429. (doi:10.1093/jhered/esab014)
25. Quinlan AR, Hall IM. 2010 BEDTools: a flexible suite of utilities for comparing genomic features. *Bioinformatics* **26**, 841–842. (doi:10.1093/bioinformatics/btq033)
26. Jühling F, Kretzmer H, Bernhart SH, Otto C, Stadler PF, Hoffmann S. 2016 Metilene: fast and sensitive calling of differentially methylated regions from bisulfite sequencing data. *Genome Res.* **26**, 256–262. (doi:10.1101/gr.196394.115)
27. Wickham H. 2016 *ggplot2: elegant graphics for data analysis*. New York, NY: Springer-Verlag. https://ggplot2.tidyverse.org.
28. Wickham H. 2023 forcats: tools for working with categorical variables (factors). R package version 1.0.0. https://github.com/tidyverse/forcats, https://forcats.tidyverse.org/.
29. Wickham H, François R, Henry L, Müller K, Vaughan D. 2025 dplyr: a grammar of data manipulation. R package version 1.1.4. https://dplyr.tidyverse.org.
30. Garnier S, Ross N, Rudis R, Camargo PA, Sciaini M, Scherer C. 2024 viridis(Lite)—colorblind-friendly color maps for R. viridis package version 0.6.5. https://sjmgarnier.github.io/viridis/ (doi:10.5281/zenodo.4679423)
31. R Core Team. 2025 *R: a language and environment for statistical computing*. Vienna, Austria: R Foundation for Statistical Computing. https://www.R-project.org/.

32. Broad Institute. 2019 *Picard toolkit*. Broad Institute, GitHub repository. http://broadinstitute.github.io/picard (accessed 23 July 2025).
33. Guo W, Zhu P, Pellegrini M, Zhang MQ, Wang X, Ni Z. 2018 CGmapTools improves the precision of heterozygous SNV calls and supports allele-specific methylation detection and visualization in bisulfite-sequencing data. *Bioinformatics* **34**, 381–387. (doi:10.1093/bioinformatics/btx595)
34. Li H 2011 Tabix: fast retrieval of sequence features from generic TAB-delimited files. *Bioinformatics* **27**, 718–719. (doi:10.1093/bioinformatics/btq671)
35. Danecek P *et al.* 2021 Twelve years of SAMtools and BCFtools. *Gigascience* **10**, giab008. (doi:10.1093/gigascience/giab008)
36. Chang CC, Chow CC, Tellier LC, Vattikuti S, Purcell SM, Lee JJ. 2015 Second-generation PLINK: rising to the challenge of larger and richer datasets. *Gigascience* **4**, s13742–015. (doi:10.1186/s13742-015-0047-8)
37. Purcell S, Chang C. PLINK v2.0.0-a.7LM AVX2. https://www.cog-genomics.org/plink/2.0/ (accessed 8 July 2025).
38. Zhou X, Stephens M. 2012 Genome-wide efficient mixed-model analysis for association studies. *Nat. Gen.* **44**, 821–824. (doi:10.1038/ng.2310)
39. Wickham H *et al.* 2019 Welcome to the Tidyverse. *J. Open Source Softw.* **4**, 1686. (doi:10.21105/joss.01686)
40. Bates D, Maechler M, Jagan M. 2010 Matrix: sparse and dense matrix classes and methods. http://cran.r-project.org/package=Matrix. (doi:10.32614/CRAN.package.Matrix)
41. Hothorn T, Bretz F, Westfall P. 2008 Simultaneous inference in general parametric models. *Biom. J.* **50**, 346–363. (doi:10.1002/bimj.200810425)
42. Bates D, Mächler M, Bolker B, Walker S. 2015 Fitting linear mixed-effects models using lme4. *J. Stat. Softw.* **67**, 1–48. (doi:10.18637/jss.v067.i01)
43. Ziyatdinov A, Vázquez-Santiago M, Brunel H, Martinez-Perez A, Aschard H, Soria JM. 2018 lme4qtl: linear mixed models with flexible covariance structure for genetic studies of related individuals. *BMC Bioinformatics* **19**, 68. (doi:10.1186/s12859-018-2057-x)
44. Lindner M, Laine VN, Verhagen I, Viitaniemi HM, Visser ME, van Oers K, Husby A. 2021 Rapid changes in DNA methylation associated with the initiation of reproduction in a small songbird. *Mol. Ecol.* **30**, 3645–3659. (doi:10.1111/mec.15803)
45. Lenth R. 2025 emmeans: estimated marginal means, aka least-squares means. (doi:10.32614/CRAN.package.emmeans)
46. Strimmer K. 2008 fdrtool: a versatile R package for estimating local and tail area-based false discovery rates. *Bioinformatics* **24**, 1461–1462. (doi:10.1093/bioinformatics/btn209)
47. Meaney MJ, Szyf M. 2005 Environmental programming of stress responses through DNA methylation: life at the interface between a dynamic environment and a fixed genome. *Dialog. Clin. Neurosci.* **7**, 103–123. (doi:10.31887/DCNS.2005.7.2/mmeaney)
48. Fox JA, Reader SM, Barrett RDH. 2025 Rapid neural DNA methylation responses to predation stress in Trinidadian guppies. *Mol. Ecol.* **34**, e17773. (doi:/10.1111/mec.17774)
49. Geetha-Loganathan P, Nimmagadda S, Pröls F, Patel K, Scaal M, Huang R, Christ B. 2005 Ectodermal Wnt-6 promotes Myf5-dependent avian limb myogenesis. *Dev. Biol.* **288**, 221–33. (doi:10.1016/j.ydbio.2005.09.035)
50. Giordani J, Bajard L, Demignon J, Daubas P, Buckingham M, Maire P. 2007 Six proteins regulate the activation of Myf5 expression in embryonic mouse limbs. *Proc. Natl Acad. Sci. USA* **104**, 11310–11315. (doi:10.1073/pnas.0611299104)
51. Gamer LW, Ho V, Cox K, Rosen V. 2008 Expression and function of BMP3 during chick limb development. *Dev. Dyn.* **237**, 1691–1698. (doi:10.1002/dvdy.21561)
52. Pinto do ÓP, Kolterud Å, Carlsson L. 1998 Expression of the LIM-homeobox gene LH2 generates immortalized steel factor-dependent multipotent hematopoietic precursors. *EMBO J.* **17**, 5744–5756. (doi:10.1093/emboj/17.19.5744)
53. Pinto do ÓP, Richter K, Carlsson L. 2002 Hematopoietic progenitor/stem cells immortalized by Lhx2 generate functional hematopoietic cells *in vivo*. *Blood* **99**, 3939–3946. (doi:10.1182/blood.v99.11.3939)
54. Rhee H, Polak L, Fuchs E. 2006 Lhx2 maintains stem cell character in hair follicles. *Science* **312**, 1946–1949. (doi:10.1126/science.1128004)
55. Subramanian L *et al.* 2011 Transcription factor Lhx2 is necessary and sufficient to suppress astrogliogenesis and promote neurogenesis in the developing hippocampus. *Proc. Natl Acad. Sci. USA* **108**, E265–E274. (doi:10.1073/pnas.1101109108)
56. Zhao Y, Mailloux CM, Hermesz E, Palkóvits M, Westphal H. 2010 A role of the LIM-homeobox gene Lhx2 in the regulation of pituitary development. *Dev. Biol.* **337**, 313–323. (doi:10.1016/j.ydbio.2009.11.002)
57. Chou SJ, Tole S. 2019 Lhx2, an evolutionarily conserved, multifunctional regulator of forebrain development. *Brain Res.* **1705**, 1–14. (doi:10.1016/j.brainres.2018.02.046)
58. Watson BA *et al.* 2018 LHX2 mediates the FGF-to-SHH regulatory loop during limb development. *J. Dev. Biol.* **6**, 13. (doi:10.3390/jdb6020013)
59. Chou SJ, O'Leary DD. 2013 Role for Lhx2 in corticogenesis through regulation of progenitor differentiation. *Mol. Cell. Neurosci.* **56**, 1–9. (doi:10.1016/j.mcn.2013.02.006)
60. Muralidharan B *et al.* 2017 LHX2 interacts with the NuRD complex and regulates cortical neuron subtype determinants Fezf2 and Sox11. *J. Neurosci.* **37**, 194–203. (doi:10.1523/JNEUROSCI.2836-16.2016)
61. Gordon PJ, Yun S, Clark AM, Monuki ES, Murtaugh LC, Levine EM. 2013 Lhx2 balances progenitor maintenance with neurogenic output and promotes competence state progression in the developing retina. *J. Neurosci.* **33**, 12197–12207. (doi:10.1523/JNEUROSCI.1494-13.2013)
62. Hägglund AC, Dahl L, Carlsson L. 2011 Lhx2 is required for patterning and expansion of a distinct progenitor cell population committed to eye development. *PLoS ONE* **6**, e23387. (doi:10.1371/journal.pone.0023387)
63. Tétreault N, Champagne MP, Bernier G. 2009 The LIM homeobox transcription factor Lhx2 is required to specify the retina field and synergistically cooperates with Pax6 for Six6 trans-activation. *Dev. Biol.* **327**, 541–550. (doi:10.1016/j.ydbio.2008.12.022)
64. Zibetti C, Liu S, Wan J, Qian J, Blackshaw S. 2019 Epigenomic profiling of retinal progenitors reveals LHX2 is required for developmental regulation of open chromatin. *Commun. Biol.* **2**, 142. (doi:10.1038/s42003-019-0375-9)
65. Alfano G *et al.* 2011 Vax2 regulates retinoic acid distribution and cone opsin expression in the vertebrate eye. *Development* **138**, 261–271. (doi:10.1242/dev.051037)
66. Alfano G, Shah AZ, Jeffery G, Bhattacharya SS. 2016 First insights into the expression of VAX2 in humans and its localization in the adult primate retina. *Exp. Eye Res.* **148**, 24–29. (doi:10.1016/j.exer.2016.05.008)
67. Barbieri AM *et al.* 1999 A homeobox gene, *vax2*, controls the patterning of the eye dorsoventral axis. *Proc. Natl Acad. Sci. USA* **96**, 10729–10734. (doi:10.1073/pnas.96.19.10729)
68. Barbieri AM *et al.* 2002 *Vax2* inactivation in mouse determines alteration of the eye dorsal-ventral axis, misrouting of the optic fibres and eye coloboma. *Development* **129**, 805–813. (doi:10.1242/dev.129.3.805)
69. Ye M, Lu Q, Zhao D, Zhao B, Zhang S, Liao Y, Liao R. 2023 New endothelial corneal dystrophy in a Chinese family. *Cornea* **42**, 529–535. (doi:10.1097/ICO.0000000000003209)
70. Fliegauf M *et al.* 2006 Nephrocystin specifically localizes to the transition zone of renal and respiratory cilia and photoreceptor connecting cilia. *J. Am. Soc. Nephrol.* **17**, 2424–2433. (doi:10.1681/ASN.2005121351)

71. Birtel J *et al.* 2021 *NPHP1* gene-associated nephronophthisis is associated with an occult retinopathy. *Kidney Int.* **100**, 1092–1100. (doi:10.1016/j.kint.2021.06.012)
72. Wolf MT, Hildebrandt F. 2011 Nephronophthisis. *Pediatr. Nephrol.* **26**, 181–194. (doi:10.1007/s00467-010-1585-z)
73. Husby A. 2020 On the use of blood samples for measuring DNA methylation in ecological epigenetic studies. *Int. Comp. Biol.* **60**, 1558–1566. (doi:10.1093/icb/icaa123)
74. Laine VN, *et al.* 2016 Evolutionary signals of selection on cognition from the great tit genome and methylome. *Nat. Commun.* **7**, 10474. (doi:10.1038/ncomms10474)
75. Lindner M, Verhagen I, Viitaniemi HM, Laine VN, Visser ME, Husby A, van Oers K. 2021 Temporal changes in DNA methylation and RNA expression in a small song bird: within- and between-tissue comparisons. *BMC Genomics* **22**, 36. (doi:10.1186/s12864-020-07329-9)
76. Siller Wilks SJ, Heidinger BJ, Westneat DF, Solomon J, Rubenstein DR. 2024. The impact of parental and developmental stress on DNA methylation in the avian hypothalamic–pituitary–adrenal axis. *Mol. Ecol.* **33**, e17291. (doi:10.1111/mec.17291)
77. Guindre-Parker S. 2020 Individual variation in glucocorticoid plasticity: considerations and future directions. *Int. Comp. Biol.* **60**, 79–88. (doi:10.1093/icb/icaa003)
78. Krueger F. 2015 Trim Galore is a wrapper around Cutadapt and FastQC to consistently apply adapter and quality trimming to FastQ files, with extra functionality for RRBS data. https://github.com/FelixKrueger/TrimGalore. (doi:10.5281/zenodo.7598955). (accessed 28 April 2025).
79. Rubenstein DR, Solomon J. 2025 Lamprotornis superbus representation bisulfite sequencing for common garden experiment. The National Center for Biotechnology Information. See https://www.ncbi.nlm.nih.gov/bioproject/?term=PRJNA1252789.
80. Rubenstein DR, Solomon J. 2025 Data from: Endocrine and epigenetic flexibility in an African starling. Dryad Digital Repository. (doi:10.5061/dryad.t4b8gtjff)
81. Rubenstein DR, Solomon J. 2026. Supplementary material from: Endocrine and epigenetic flexibility in an African starling. Figshare. (doi:10.6084/m9.figshare.c.8555982)